Optics & Laser Technology 44 (2012) 130–135

Contents lists available at ScienceDirect

Optics & Laser Technology

journal homepage: www.elsevier.com/locate/optlastec

Design and construction of Q-switched Nd:YAG laser system for LIBS measurements

Khaled. Elsayed [a,*], Hisham Imam [b], Amro Harfoosh [b], Yasser Hassebo [d], Yasser Elbaz [b], Mouayed Aziz [b], Mohy Mansour [c]

[a] Physics Department, Faculty of Science, Cairo University, Giza 12211, Egypt
[b] National Institute of Laser Enhanced Sciences, Cairo University, Giza 12211, Egypt
[c] Mechanical Power Engineering Department, Faculty of Engineering, Cairo University, Giza 12211, Egypt
[d] Mathematics/Engineering Department, LaGuardia Community College of the City University of New York, 31-10 Thomson Avenue, Long Island City, NY 11101, USA

ARTICLE INFO

Article history:
Received 27 March 2011
Received in revised form
14 June 2011
Accepted 14 June 2011
Available online 6 July 2011

Keywords:
LIBS technique
Nd:YAG laser
Passive Q-switch

ABSTRACT

A passive, Q-switched pulsed, Nd:YAG laser system was designed and built, which can provide a potential compact robust laser source for portable laser induced breakdown spectroscopy systems.

The developed laser system operates at 1064 nm. Each laser shot contains a train of pulses having maximum total output energy of 170 mJ. The number of pulses varies from 1–6 pulses in each laser shot depending on the pump energy. The pulse width of each pulse ranges from 20 to 30 ns. The total duration of the output pulse train is within 300 μs. The multi-pulse nature of the laser shots was employed to enhance the LIBS signal. To validate the system, LIBS measurements and analysis were performed on ancient ceramic samples collected from Al-Fustat excavation in Old Cairo. The samples belong to different Islamic periods in Egypt history. The results obtained are highly indicative that useful information can be provided to archeologists for use in restoring and repairing of precious archeological objects.

1. Introduction

Laser-induced breakdown spectroscopy (LIBS) is an emerging atomic emission spectroscopic technique that offers the prospect of highly selective, sensitive, real-time detection and analysis of both natural and man-made materials [1,2]. The ability to obtain rapid, multi-elemental, in-situ analysis represents a unique advantage of LIBS over other analytical techniques. In recent years, the need for compact portable LIBS systems for a variety of applications such as military, home security, archeology, and environmental applications has increased.

Many research efforts have been focused on methods to further elucidate and improve the LIBS analytical response. Double pulse is one of the techniques used for enhancing LIBS signal and generating more intense plasma emission due to its sensitivity and stable emission signal that can produce manifold signal intensities with respect to conventional LIBS for metallic targets kept in a gaseous environment or placed under water [3–8]. The double pulse LIBS technique uses two laser impulses separated by some delay, of the order of microseconds.

In this study, a multipulse, passively Q-switched, Nd:YAG laser system was designed and built. This system can provide a potential compact robust laser source for portable laser induced breakdown spectroscopy system [9]. The passive Q-switching technique was chosen while designing the system for more compactness, and to generate multi-pulses in each laser shot. Unlike the single-pulse Q-switched lasers, the radiation emitted by multipulse passive Q-switched (MPQ) lasers could be easier to couple through optical fibers to the target by properly selecting the working regime. The high intensity reached at the input face of the fiber would be reduced in the case of the MPQ, which in turns prevent exceeding damage threshold of the fiber.

The system was used in LIBS experiments on archeological samples that were collected from Al-fustat excavation in old Cairo belongs to different Islamic periods in Egypt to determine the elemental composition of samples. The information extracted would enable the archeologists to have useful information about ancient technology and evaluating the firing conditions and temperatures while they were manufacturing pottery. Accordingly this will help in restoring and repairing of the precious archeological objects. The results obtained are highly indicative and show a reasonable agreement with the emission spectra obtained from a commercial Nd:YAG laser system.

2. Laser system design and characterization

One of the possibilities to improve LIBS data is to use two laser pulses separated by some delay, on the order of microseconds [10]. The observed signal enhancement is attributed to plasma

* Corresponding author.
E-mail address: kelsayed@niles.edu.eg (Khaled. Elsayed).

0030-3992/$ - see front matter © 2011 Elsevier Ltd. All rights reserved.
doi:10.1016/j.optlastec.2011.06.005

re-heating. However, the disadvantage of the analytically promising double-pulse approach is that it uses a complicated experimental setup based on the use of two synchronized and carefully aligned laser sources, a requirement, which largely inhibits its practical application. Having a laser source that can provide multiple pulses within each laser shot is an advantage. The use of pulse trains by using passive Q-switch, produce higher emission intensities and betters signal noise ratio. The enhancement can rather be explained by a substantial increase in plasma temperature (re-heating) caused by the efficient absorption of the consecutive multiple infrared laser pulses by the plasma core. Most of the energy of later coming laser pulses is mainly exploited for re-heating and breaking down of the matter ablated by the first pulse (s) of the laser shot, instead of increasing the ablation rate [23]. The disadvantage of using multipulse by using passive Q-switch laser is the lacking of the control of the delay between laser pulses in the single laser shot.

The present Nd:YAG laser system was designed to meet the following requirements:

i. Able to deliver peak power greater than that needed for breakdown threshold.
ii. Multi-pulse laser source since multi-pulse laser system enhance the signal intensities.
iii. Provide a potential compact, robust laser source for portable LIBS system.

Based on information regarding the breakdown threshold of solid targets in related literature [1,3], a single passive laser shot contains train of required pulses. Each pulse should be in the range of 1 MW/cm^2. Assuming the pulse width of the passive Q-switch is in the range of nanoseconds, and the energy of each pulse is about or more than 25 mJ; the total Q-switched energy of each shot should be in the range of 100–170 mJ.

Based on analogous design, a 60 mm length Nd:YAG laser rod with diameter of 4 mm is chosen. The arc length of the flashlamp is 50 mm with bore diameter, $d=3$ mm. The flashlamp is pumped with a long pulse width ($tp=900$ μsec) in order to increase its lifetime.

Knowing that the efficiency of the Nd:YAG laser system ranges from 1–2%, the flashlamp driving circuit should be able to provide 50 J.

A single mesh driving circuit was chosen for the flashlamp. Fig. 1 shows the flashlamp driver circuit that designed based upon the above calculated parameters.

In this circuit, a half wave voltage doubler was chosen. The circuit consists of the bank capacitor (C_2), charging capacitor (C_1) and the diodes D_1 to D_4. The 350 VAC at point A is doubled to 700 VDC and raised to about 1 kV at point B. The voltage at point C is about 500 VDC, this voltage charges the capacitor C_3 through R_3. This capacitor is discharged through the primary coil of T_1 (L_1) and raised to about 10 kV as a trigger pulse through the flashlamp by the secondary L_2. The power transformer, which has a secondary coil of two taps give 350 and 175 VAC, therefore one can select, after doubling, two charging values, Vo∼1.0, 0.5 kv. The bank capacitor consists of four capacitors connected in series to give $C_{bank}=101$ μF/2kv. The inductor L_2 is the secondary of the series triggering transformer (T_1). Its value is 99 μH. The triggering technique is therefore a series triggering. The trigger pulse at the primary of the transformer is obtained using the voltage divider. The capacitor C_3 is charged via charging resistor R_3.

The single mesh PFN circuit parameters have been calculated according to the equations given in Ref. [11]. Values of components of the flashlamp driving circuit are as follows in Table 1:

A single ellipsoidal pump cavity was chosen as this pumping configuration and yields a high coupling efficiency [12]. The reflector material is brass coated with gold.

The Nd:YAG resonant cavity consists of two 6 mm diameter flat mirrors, M_1 and M_2, on both sides of the gain medium as shown in Fig. 2. This represents a plane-parallel cavity configuration, which is very useful for pulsed solid state lasers because of its large mode volume. However, the disadvantage of the plane parallel cavity is some difficulty in alignment. This difficulty was overcome by the use of a short resonator length (80 mm), which is also needed for compactness.

The maximum output pulse energy of the Nd:YAG laser system was measured using an optical power meter (Ophire Nova, Ophir Optronics Ltd.). Three output couplers were used for the present work with reflectivities of 50%, 60% and 70%. The maximum output energy was obtained was 170 mJ at output reflectivity of 50%.

Table 1

Component	Value
C_1	0.2 μF/600 v
C_2	101 μF/2.0 kv
L_2	99 μH (60 turns) Øw2=1.5 mm
L_1	(3 turns) Øw1=1.5 mm
D_1–D_4	1N5408
C_3	0.47 μF/600 V
R_1 and R_2	150 kΩ/1 W
R_3	10 kΩ/1 W

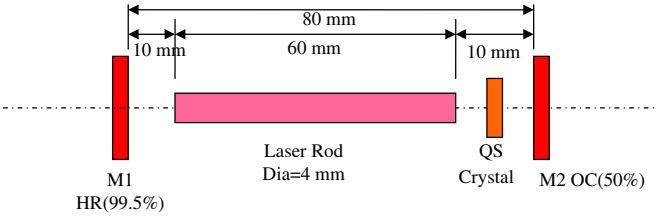

Fig. 2. Layout of the laser resonator.

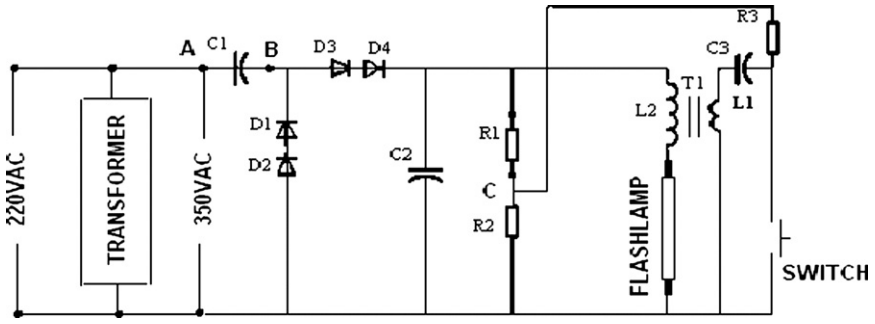

Fig. 1. Flashlamp driving circuit.

The temporal profile of the system has been measured by using a digital oscilloscope and ultra-fast photodiode UPD-200-VD (rise time 200 ps ,190–1100 nm). This is shown in Fig. 3.

The output, a passive Q-switched train of pulses (1–6 pulses) from a single shot, is shown in this figure. The number of pulses was found to be in the range of 1–6. By increasing the pump energy, the number of pulses per shot increases. The six laser pulses are obtained at the maximum pump energy of 50 J. The pulse width of each pulse ranges from 20 to 30 ns. All laser pulses in each shot have different intensities. The variation of the laser pulse energy in each shot is within 36% relative standard deviation.

The minimum energy per pulse within train of pulses is 10 mJ while the maximum is 60 mJ. The average energy per pulse is 28 mJ. The maximum total energy of the 6- pulses laser shot is approximately 170 mJ with 16% relative standard deviation.

The pulses are found to be relatively evenly distributed in time. The total duration of the output pulse series is within 300 μs. The inter-pulse time gap at the maximum pump energy is 60 μs. At any given pump energy level, the laser output pulse structure was seen to be reasonably stable; only one out of 10–20 shots gave rise to a pulse number one higher or lower .The jitter on the time gaps between pulses was found to be 3–5 μs. The inter-pulse time gap between the last two pulses was about 25% shorter than all former gaps. Output peak power of Q-switched pulse is $\cong 1$ MW. When such laser pulse is focused to spot size of 600 μm diameter, the irradiance of the laser pulse will reach 0.35 GW/cm^2, which is more than the breakdown threshold of the solid targets [3]. The overall laser system is shown in Fig. 4.

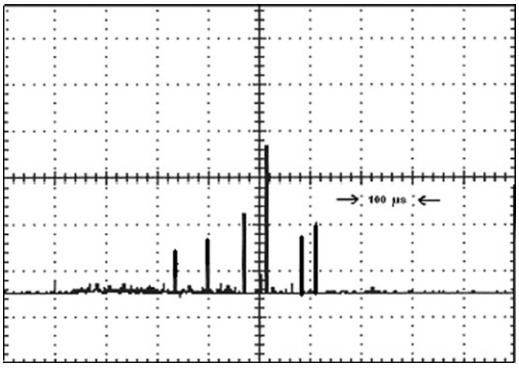

Fig. 3. Temporal profile of passively Q-switched laser pulses.

3. Experimental

The home-made MPQ Nd:YAG laser system was used in a LIBS experiment to determine the elemental compositions of different ceramic samples The schematic diagram of laser induced LIBS experimental setup is shown in Fig. 5.

It consists of our experimentally developed single shot passively Q-switched Nd:YAG laser system. The laser beam was focused onto the sample surface in a perpendicular direction via a quartz plano-convex lens of 25 cm focal length to produce high power density, which is necessary to produce breakdown. The spot size diameter (crater) of the focused laser beam was about 600 μm. At this spot size diameter, the power density reaches 0.35G W/cm^2.

The emitted light from the plasma plume was collected via 200 μm diameter, one-meter length wide band fused-silica optical fiber connected at its other side to an echelle spectrometer. The PI-Echelle provides a constant spectral resolution of 3100 corresponding to 4 pixels FWHM, over a wavelength range 190–1100 nm displayable in a single spectrum (Princeton Instrumentation, Acton, SE200PI-HO). ICCD camera (PI-Max), coupled to the spectrometer was used for detection of the dispersed light.

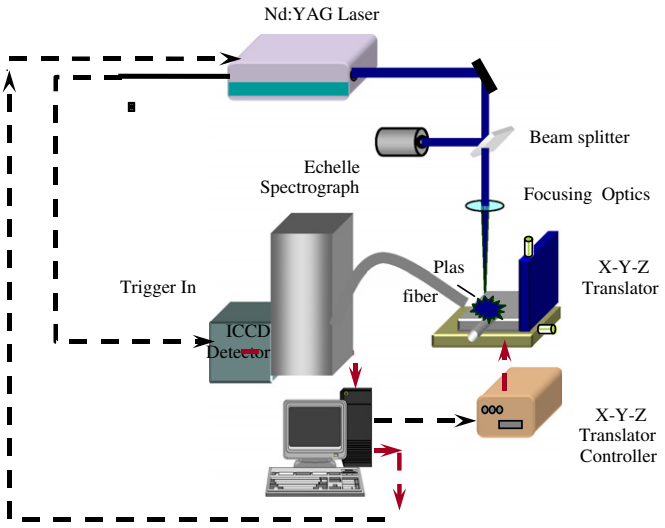

Fig. 5. LIBS experimental setup.

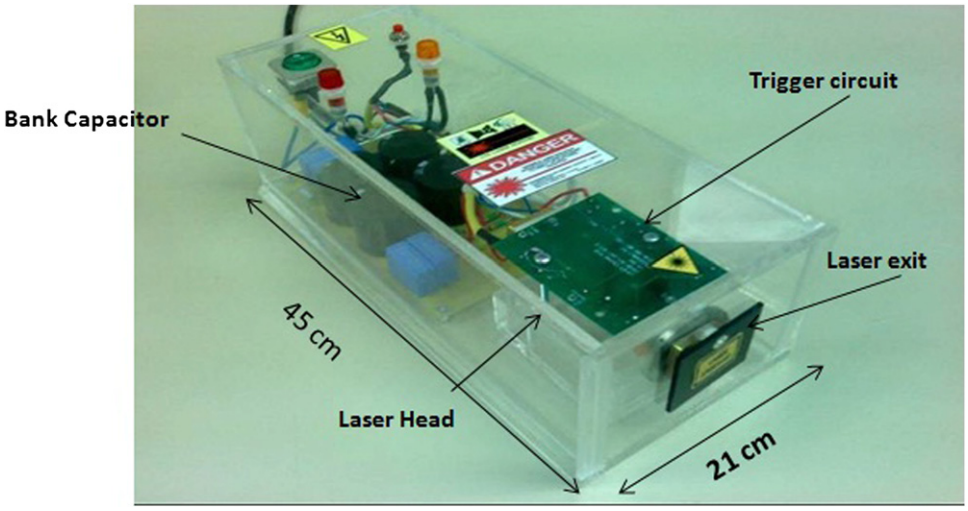

Fig. 4. The passive Q-switched pulsed Nd:YAG laser system.

To improve LIBS precision, spectra from several laser shots were averaged in order to reduce statistical error due to laser shot-to-shot fluctuation. The measurements were reproduced at five locations on the sample surface in order to avoid problems linked to sample heterogeneity. Twenty laser shots were fired at each location and saved in separated files and the average (average of 100 spectra) was computed and saved to serve as the library spectrum. The plasma emission spectra were collected under atmospheric pressure. Spectral lines were identified using atomic spectra data base of GRAMS software V8.0.

3.1. Archeological ceramic samples:

The samples were collected from Al-Fustat excavation in Old Cairo. Fig. 6 shows a collection of these samples.

3.2. Results and discussion

Selected spectra from clay bodies of Fatimid samples are shown in Fig. 7. As shown from the characteristic emission lines in this spectrum, the clay bodies of these samples contain a relatively high ratio of calcium, this indicates that the clay used was calcareous clay. These results show that the ceramic objects are often made from local clay sources [13–15].

Selected spectra from clay bodies of Mamlouki samples are shown in Fig. 8. As shown from the characteristic emission lines in this spectrum, the clay bodies of these samples contain a relatively high contains of iron (Fe). This indicates that the clays used in these samples were iron clay. Iron-rich minerals, with the iron primarily in the form of hematite Fe_2O_3, goethite (FeOOH) have been found in the clay bodies of Mamlouki samples [13].

The analytical measurements in the present study were carried out under local thermo-dynamic equilibrium (LTE) conditions. To verify the LTE we must estimate, the electron density *Ne* and electron temperature *Te*, and study the temporal behavior of them with dynamic processes.

Fig. 6. Samples from different periods.

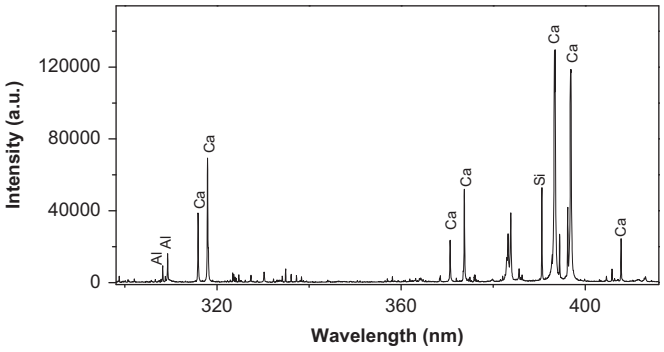

Fig. 7. Emission spectra from Fatima ceramic body of archeological samples.

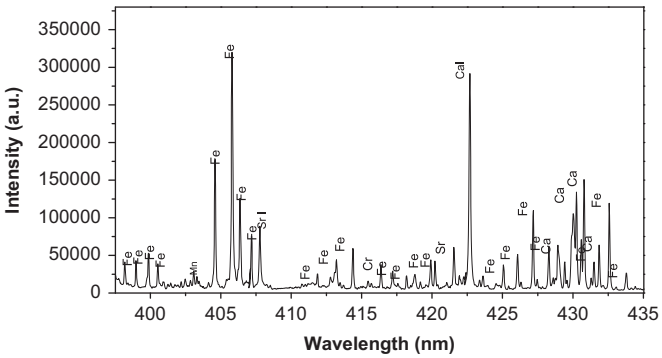

Fig. 8. Emission spectra from Mamlouki brown ceramic body of archeological samples.

One of the most powerful spectroscopic techniques to determine the electron density with reasonable accuracy is the measurement of the Stark broadening profile of the atomic emission lines. In the present experiment, we choose for electron density measurements the Ca I transition at 452.69 nm [15]. Stark broadening of spectral lines in plasmas is the effect of the collisions with charged species, resulting in both a broadening of the spectral line and a shift in the peak wavelength. The electrons in the plasma can perturb the energy levels of the individual ions, which broaden the emission lines originating from excited levels. Stark broadening of well-isolated lines in the plasma is, thus, useful for estimating the electron densities provided that the Stark broadening coefficients are given. Several Stark broadening coefficients have been listed by Griem [16].

The FWHM of the Stark broadened lines $\Delta\lambda_{1/2}$ is related to the electron density by the expression (for singly ionized ions):

$$\Delta\lambda_{1/2} = 2w\left(\frac{N_e}{10^{16}}\right) + 3.5A\left(\frac{N_e}{10^{16}}\right)^{1/4}(1-1.2N_D{}^{-1/3})w\left(\frac{N_e}{10^{16}}\right)\text{Å} \quad (1)$$

The first term in Eq. (1) gives the contribution from electron broadening, and the second term is the ion broadening correction. *w* is the electron impact parameter, which can be interpolated at different temperatures, and *A* is the ion broadening parameter. Both *w* and *A* are weak functions of temperature [16]. Ne is the electron density (cm^{-3}) and ND the number of particles in the Debye sphere (see Refs. [16,17]) given by

$$N_D = 1.72 \times 10^9 \frac{T_e{}^{3/2}(\text{eV})}{N_e{}^{1/2}(\text{cm}^{-3})} \quad (2)$$

The contribution from quasi-static ion broadening (the second term of Eqs. (4)–(1) is small in our case. Its value can be evaluated from the extrapolation of the Griem estimation for *A* and *w* (for *Te*=8000 K and *Ne*~1017 cm^{-3}, its contribution is less than 2%). Neglecting this contribution, Eq. (1) can be reduced to

$$\Delta\lambda_{1/2} = 2w\left(\frac{N_e}{10^{16}}\right)\text{Å} \quad (3)$$

The observed line shape was corrected by simply subtracting the contribution of the instrumental line broadening through the relation [18,24]

$$\Delta\lambda_{true} = \Delta\lambda_{observed} - \Delta\lambda_{instrument} \quad (4)$$

In our case $\Delta\lambda_{instrument}$ was found to be 0.06 nm as determined by measuring the FWHM of the narrow He–Ne laser line at 632.6 nm. Line width, determined by numerical fitting of a Lorentzian profile to the measured line profiles, shows some dependence on the lateral position in the plasma, usually about 20–30% of the maximum FWHM, which is in qualitative agreements with Andreic et al. [19].

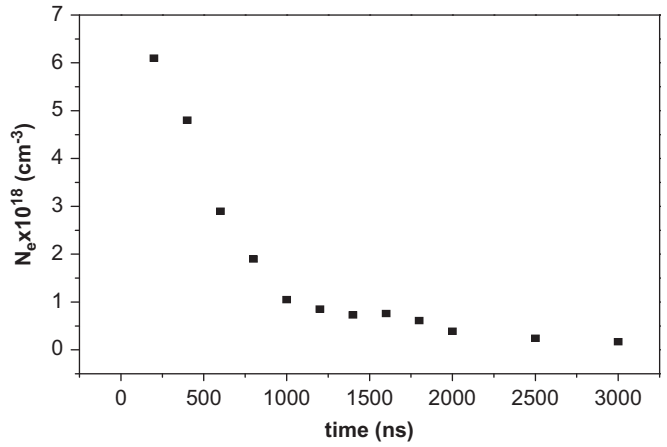

Fig. 9. Electron density temporal evolution (*Ne*).

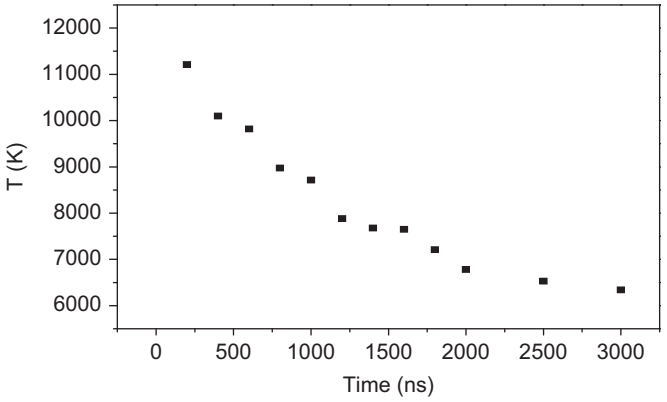

Fig. 10. Temporal behavior of the plasma temperature obtained via Boltzmann equation.

The temporal evolution of the electron density deduced from the Stark broadening of Ca I 452.69 nm is shown in Fig. 9.

The temporal evolution of *Ne* is found to diminish exponentially with time and then level off. The fast decay rate of electron density can be attributed to the plasma expansion, while the slowing and leveling off at longer times are probably due to recombination.

The plasma temperature can be calculated from the relative line intensity of the same element. The measured intensity combined with Boltzmann equation to determine the excitation temperature of the plasma. The plasma temperature has been determined by the Boltzmann pair line method for the same species that have the same stage of ionization as demonstrated by the following Eq. (5) [16,20]:

$$\frac{I_1}{I_2} = \frac{g_1}{g_2}\frac{A_1}{A_2}\frac{\lambda_2}{\lambda_1}\exp\left(\frac{-|E_2 - E_1|}{KT_e}\right) \quad (5)$$

The two Ca lines at 452.69 nm (E=43 933 cm^{-1}) and 430.77 nm (E=38 417 cm^{-1}) for relevant spectral segments were used.

Plasma temperature values are plotted as a function of gate delay as shown in Fig. 10. It can be observed that the plasma temperature decreases exponentially by increasing the gate delay with slow variation as shown in Fig. 10, e.g. from 11223.54 to 7965.28 K° at 200 ns and 1200 ns, respectively. The temperature decreases with increasing the gate delay enhances further recombination rate as mentioned above.

The analytical measurements in the present study were carried out under local thermo-dynamic equilibrium (LTE) conditions. Thermal equilibrium means that all processes in plasma are collision-dominated and the plasma can be described by single temperature parameter, i.e. *Te*=*Ti*.

In fact, at shorter times after the onset of the laser-breakdown, the fast dynamics of the plasma does not allow for the system to reach thermo-dynamic equilibrium, so that the relative concentrations of the different species in the plasma cannot be described with just a single temperature as it should be in the framework of the LTE theory. Moreover, immediately after the onset of the laser breakdown, radiative processes such as spontaneous emission, reabsorption and stimulated emission are predominant over the collisional effects, thus invalidating the LTE approximation. Conversely, at longer times the electron density in the plasma is low, so that the thermal equilibrium between the plasma species cannot be sustained by the electron–ion collisions. At low values of the electron density the three-body recombination effect has also to be taken into account. All these effects lead to the violation of the LTE approximation, thus giving apparently different plasma temperatures when considering the different species in the plasma.

The simple criterion of McWhirter formula given by Eq. (5) has been applied for judging the existence of LTE in the present work. Substituting in Eq. (5) with the temperature values previously calculated from Boltzmann equations, a value for the electron density (*Ne*) less than electron density calculated from Stark method is obtained, which means that the LTE conditions is valid over a range of delay.

As pointed out in the original publication [21], that McWhirter formula is necessary but not sufficient for the validity of the LTE assumption in case of laser-induced plasma, therefore two additional criteria should be verified for LTE validity especially for transient and inhomogeneous plasma as mentioned by Griem [16]. In the present work, the obtained plasma assumed to be homogeneous according to the confinement effect, therefore only the transient plasma condition needs to be verified. However, the present plasma parameters are varied with small change over the selected experimental parameter, i.e. gate delay, and McWhirter criterion is fulfilled that means the plasma evolves through quasi equilibrium near LTE states. Nevertheless, for successfully checked LTE plasma, transient plasma criterion is needed to the validity of LTE, which states that the relaxation time of plasma (time needed for the establishment of excitation and ionization equilibrium) is shorter than the variation time of plasma parameters. This can be true locally and for specific time region in the plasma evolution corresponding to its dynamic expanding characteristic [22].

The data indicates that the laser, used in these measurements, has peak power greater than that needed for breakdown threshold and it is appropriate for LIBS application.

The presented compact and robust passive Q-switched Nd:YAG laser system has a high potential to be used in portable LIBS system to identify and analyze archeological objects in stiu.

4. Conclusions

The design, construction and operation of a multipulse passive Q-switched Nd:YAG laser system has been presented. This system provides a potential compact robust laser source for portable LIBS system. This is an advantage since most other analytical techniques cannot be easily used in field operations.

A train of (1–6) output Q-switched pulses is obtained from a single shot. The width of each pulse ranges from 20 to 30 ns. The minimum energy per pulse within train of pulses is 10 mJ while the maximum is 60 mJ. The average energy per pulse is 28 mJ. The maximum total energy of the 6- pulses laser shot was about 170 mJ obtained at the maximum pump energy of 50 J.

The laser system was used in LIBS experiment on archeological samples that were collected from Al-fustat excavation in old Cairo belongs to different periods in Egypt to determine the elemental composition of samples. The analytical measurements in the present study were carried out under local thermo-dynamic equilibrium (LTE) conditions. To verify the LTE we estimated, the electron density *Ne* and electron temperature *Te*, and studied the temporal behavior of them with dynamic processes. This enables the archeologists to have useful information about ancient technology and evaluating the firing conditions and temperatures during the manufacturing of ancient pottery samples. Accordingly this will help in restoring and repairing of the precious archeological objects. The data indicates that the laser used in these measurements is appropriate for LIBS application.

References

[1] Cremers DA, Radziemski LJ. Hand Book of Laser Induced Breakdown Spectroscopy. New York: Wiley; 2006.
[2] Yueh F, Singh JP, Zang H, Meyers RA, editors. Encyclopedia of Analytical Chemistry. John Wiley and sons ltd; 2000.
[3] St-Onge L, Detalle V, Sabsabi M. Spectrochim Acta Part B 2002;57:121–35.
[4] Babushok VI, Delucia Jr FC, Goltfried JL, Munson CA, Miziolek AW. Spectrochim Acta part B 2006;61:999–1014.
[5] Hohreiter V, Hahn DW. Spectrochim Acta part B 2005;60:968–74.
[6] Scott RH, Strasheim A. Spectrochim Acta Part B 1970;25:311–32.
[7] Cremers DA, Radziemski LJ, Loree TR. Appl Spectrosc 1984;38:721–9.
[8] Noll R, Sattmann R, Sturn V, Winkelmarm S. J Anal At Spectrom 2004;19:419–28.
[9] Singh JP, Thakur SN, editors. Laser Induced Breakdown Spectroscopy. Elsevier; 2007.
[10] De Giacomo A, Dell'Aglio M, De Pascale O, Capitelli M. Spectrochim Acta Part B: At Spectrosc 2007;62(8):721–38.
[11] Koechner W. Solid-State Laser Engineering. 5th ed. Berlin: Springer; 1999.
[12] Siegman AE. Lasers. California: University Science Books; 1986.
[13] Rice PM. Pottery Analysis: A Sourcebook. The University of Chicago and London; 1988.
[14] Thierrin – Michel, G. Fourth Euro-Ceramics, vol. 14, The Cultural Ceramics Heritage. In: Proceedings of the 3rd European Meeting on Ancient Ceramics. Faenza, Italy: C.N.R. IRTEC; 1995. p. 173–83.
[15] Downi CA. Glaze Analysis of 15th to 17th Century Islamic Ceramics from the Collection of the Arthur M. Sackler Gallery. Kingston, Ontario, Canada: Queens University; 2002.
[16] H. R. Griem, Plasma Spectroscopy, Mc Graw-Hill New York. (1964).
[17] Lochte-Holtgreven W, editor. Plasma Diagonistics. North Holland Publishing Company; 1968.
[18] Griem HR. Spectral Line Broadening by Plasma. New York: Academic Press; 1974.
[19] Andreic Z, Henc V, Kunse HJ. Phys Scr 1993;47:405.
[20] Miziolek AW, Palleschi V, Schechter I, editors. LIBS, Fundamentals and Applications. New York: Cambridge University Press; 2006.
[21] McWhirter RWP, In: Huddlestone RH, Leonard SL, editors. Plasma Diagnostic Techniques. New York:Academic Press, 1965. p. 201–64 [chapter 5].
[22] Cristoforetti G, De Giacomo A, Dell'Aglio M, Legnaioli S, Tognoni E, Palleschi V, et al. Spectrochim Acta Part B 2010;65(86–95).
[23] St.-Onge L, Sabsabi M. Spectrochim Acta Part B 2002;57:121–35.
[24] Sabsabi Mohamad, Cielo Paolo. Appl Spectrosc 1995;49:499–507.